Earthquake Engineering, Tenth World Conference © 1992 Balkema, Rotterdam. ISBN 90 5410 060 5

Ground motion analysis using dynamic stochastic finite element method

H. Ukon, Y. Okimi, T. Yoshikiyo & T. Matsumoto
Information Processing Center, Kajima Corporation, Japan

ABSTRACT: This paper concerns stochastic behaviors of ground motion during earthquake. To numerically represent the ground motion for seismic evaluation of structures, the authors have developed dynamic stochastic finite element method using the interpolation function method. Taking a basic model and practical model with stochastic viscous boundaries as analytical examples, stochastic numerical representation of ground motion during earthquake is obtained in a form of the cross spectral function.

1. INTRODUCTION

Stochastic evaluation of structural systems in dynamic problem has been the focus of attention for these decades (Crandall 1963, Lin 1967, Nigam 1983). The stochastic finite element method proposed by Nakagiri and Hisada (Hisada 1981, 1985) is an effective and robust evaluation technique for static stochastic problems because the first or second approximation is enough to apply the static problems. But the method is not available for dynamic problem in which dominant frequency of structures changes due to the variation of structural parameters such as Young's modulus or the unit mass. The authors have proposed stochastic dynamic analysis method using finite element method (Ukon 1988) in which the interpolation function method is used instead of the perturbation technique. Complex fractional function similar to the frequency response function of a SDOF system is used as an interpolation function in the method. This technique enables us to approximate strong non-linear behavior (resonance) along structural parameter axes which are supposed to be probabilistic.

Stochastic evaluation of soil-structure systems during earthquake is another difficult problem because some consideration to boundary condition is necessary. The authors tried to apply the interpolation function method to stochastic evaluation of soil- structure systems during earthquake (Ukon 1990). Stochastic viscous boundary which is just the same as Lysmer's viscous boundary in deterministic analysis was proposed and the method was proved to have a possibility to be applied to practical problems.

Using the interpolation function method, statistic values such as the mean or the variance of time history response can be obtained in our previous study. But the frequency transfer function is quite important to discuss dynamic behaviors of a system, so the change of the frequency transfer function is highly focused on in this study instead of time history. Ground motion during earthquake is taken as the response of soil structure and it is evaluated by the cross spectral matrix. The final results of this study are the statistic values of the cross spectral matrix of response among arbitrary degrees of freedom in the soil structure. Following a brief summary of analysis, two numerical examples, a basic and a practical one, are presented in this study.

2. SUMMARY OF ANALYSIS

2.1 *Frequency transfer function*

The equation of motion of a system with viscous boundary subjected to the unit harmony acceleration $e^{i\omega t}$ is given as follows;

$$[M]\{\ddot{y}\} + [K]^{*}\{y\} = -[M]\{V\}e^{i\omega t} + [T]^{t}[D]\left(\{y_f\} - [T]\{y\}\right) \quad (1)$$

where $[M]$: the mass matrix,
$[K^{*}]$: the complex stiffness matrix,
$\{y\}$: the relative displacement vector,
$\{V\}$: the indicating vector of input direction,
$[D]$: the viscous coefficient matrix,
$[T]$: the transformation matrix,
$\{y_f\}$: the relative displacement of the free field.

Supposed $\{y\}$ in eq.(1) is given in a form of the harmony response, the frequency transfer function $\{H(\omega)\}$ is obtained in a linear form as follows;

$$\begin{aligned}\{H(\omega)\} &= \left[-\omega^{2}[M] + i\omega[T]^{t}[D][T] + [K]^{*}\right]^{-1} \\ &\quad \times \left[-[M]\{V\} + i\omega[T]^{t}[D]\{H_f\}\right] \\ &= [K_T]^{-1}\{f_T\} \end{aligned} \quad (2)$$

where $[K_T]$: the equivalent stiffness matrix,
$\{f_T\}$: the equivalent force vector,
$\{V\}$: the indicating vector of input direction,
$\{H_f\}$: the frequency transfer function of the relative displacement of the free field.

2.2 *First-order derivative*

The first-order derivative of $[K_T]$ and $\{f_T\}$ with respect to Young's modulus E_i in an irregular zone, for example, are given as follows;

$$[K_T]^{\mathrm{I}}_{E_i} = \frac{\partial [K_T]}{\partial E_i} = \frac{\partial [K]^*}{\partial E_i}, \quad \{f_T\}^{\mathrm{I}}_{E_i} = \frac{\partial \{f_T\}}{\partial E_i} = 0 \qquad (3)$$

Superscript I denotes the first-order derivative and subscript E_i means the derivative with respect to E_i.

The first-order derivative of $[K_T]$ and $\{f_T\}$ with respect to Young's modulus E_f in the free field, for example, are given as follows;

$$[K_T]^{\mathrm{I}}_{E_f} = \frac{\partial [K_T]}{\partial E_f} = i\omega \frac{\partial [D]}{\partial E_f} = i\omega \begin{bmatrix} \dfrac{\partial(\rho V_P A)}{\partial E_f} & 0 \\ 0 & \dfrac{\partial(\rho V_S A)}{\partial E_f} \end{bmatrix},$$

$$\{f_T\}^{\mathrm{I}}_{E_f} = \frac{\partial \{f_T\}}{\partial E_f} = \left(\frac{\partial [D]}{\partial E_f} \{H_f\} + [D] \frac{\partial \{H_f\}}{\partial E_f} \right) \qquad (4)$$

where V_P : the primary wave velocity,
V_S : the shear wave velocity.

2.3 *Interpolation function method*

Complex fractional functions are used to interpolate probabilistic variables instead of linear or second-order polynomials in the perturbation method. The complex function with a probabilistic variable α_i is set similar to the frequency transfer function of a SDOF system, in general, in the following form.

$$H(\omega\,;\alpha_i) = \frac{c_1 + c_2\alpha_i}{1 + c_3\alpha_i} \qquad (5)$$

where c_1, c_2, c_3 : complex or real constants.

2.4 *Cross spectral matrix of response*

Denoting the frequency transfer function matrix by $[H]$, the cross spectral matrix of input by $[G]$ and the cross spectral matrix of response by $[Z]$, then $[Z]$ is given as follows;

$$[Z] = [H]^*[G][H] \qquad (6)$$

$[H]^*$ is the complex conjugate of $[H]$. Denoting the total DOFs of a system by N, the total DOFs of input points by n, then $[H]$ is $n \times N$ matrix, $[G]$ is $n \times n$ matrix and $[Z]$ is $N \times N$ matrix. Considering an arbitrary pair of two points in the system and denoting them by p and q, then the cross spectral matrix of response between p and q is obtained by eq.(6) in a form of 2×2 matrix which is a function of frequency.

Using the mean and the first-order derivative of the frequency transfer function, each probabilistic variable can be approximated by the interpolation function method. With the power spectral density of input, G_0 and the probabilistic density function of α, $f_A(\alpha)$, the mean and the variance (or the standard deviation) are obtained by the moment calculation of a probabilistic variable. For example, the mean and the variance of the auto spectral function of response at p which is a (1,1) component of the matrix are obtained as follows;

$$E\,[Z(1,1)] = \int_{-\infty}^{\infty} H_p^* H_p G_0 f_A(\alpha)\, d\alpha \qquad (7)$$

$$Var\,[Z(1,1)] = \int_{-\infty}^{\infty} \left(H_p^* H_p G_0 - E\,[Z(1,1)] \right)^2 f_A(\alpha)\, d\alpha \qquad (8)$$

In the same manner, the mean and variance of the cross spectral function of response between p and q are obtained as follows;

$$E\,[Z(2,1)] = \int_{-\infty}^{\infty} H_p^* H_q G_0 f_A(\alpha)\, d\alpha \qquad (9)$$

$$Var\,[Z(2,1)] = \int_{-\infty}^{\infty} \left(H_p^* H_q G_0 - E[Z(2,1)] \right)^2 f_A(\alpha)\, d\alpha \qquad (10)$$

2.5 *Evaluation of correlation*

The overall variance can be obtained using each elemental variance by eq.(7) to eq.(10) *etc.*. But it can not be obtained by the simple summation of each variance because the frequency transfer function has a strong non-linearity to the change of Young's modulus and the unit mass. It is infered that the overall variance with correlational effect can be obtained by using a specific interpolation function corresponding to correlational coefficients. Then the following first-order derivative with respect to α_i was intuitively used in our previous study.

$$\{\mathbf{H}\}^{\mathrm{I}}_{\alpha_i} = \{H\}^{\mathrm{I}}_{\alpha_i} + \sum_{j=1(j\neq i)}^{NE} \{H\}^{\mathrm{I}}_{\alpha_i} E\left[\alpha_i, \alpha_j\right] \qquad (11)$$

where $\{\mathbf{H}\}^{\mathrm{I}}\alpha_i$: the modified first-order derivative,
NE : the total number of element,
$E[\alpha_i, \alpha_j]$: the correlation matrix.

After several numerical study, it is found that evaluation of correlation by eq.(11) sometimes causes lack of numerical stability when the stochastic viscous boundary is considered or the degree of randomness is high (COV is over 40%) and this is derived from the determination of the interpolation function by eq.(5) with eq.(11). So the complex constant only relating to frequency (c_3 for the unit mass) is fixed, then better stable results have been obtained. But there are still several numerical difficulties to be settled down.

3. NUMERICAL EXAMPLES

Basic examinations with the verification by Monte-Carlo simulation were reported in the references (Ukon 1988). So other two numerical examples are presented in this paper. The one is a simple finite element model which shows basic performance of the proposed method. The other is a simple and practical finite element model which shows possibility to apply the method to aseismic design analysis, vibration control analysis or stochastic ground motion analysis.

3.1 *Basic example and approximation performance*

The finite element model which consists of 26 elements and 38 nodes in this numerical example is shown in Figure 1. Analytical area is 50.0(m) in width and 25.0(m) in depth. Both free fields consist of 5 layers.

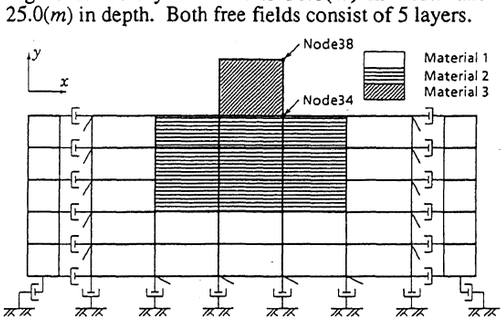

Figure 1. Basic finite element model.

Table 1. Material properties in the basic example.

Material No.	Young's modulus (kN/m^2)	Poisson's ratio	Unit mass (kg/m^3)	Damping factor
1	2.06×10^5 (0.2)	0.3 (0.2)	1.7×10^3 (0.2)	0.03 (0.2)
2	2.06×10^6 (0.2)	0.3 (0.2)	2.0×10^3 (0.2)	0.03 (0.2)
3	2.06×10^7 (0.2)	0.2 (0.2)	2.5×10^3 (0.2)	0.01 (0.2)

The model has three materials. Used material properties are summarized in Table 1. For kind of random variables are considered and the values in the parentheses are the coefficient of variation(COV). COVs in the free fields are supposed to be the same as material No. 1. The total number of the random variables is 144. Each random variable is supposed to be perfectly uncorrelated. Input motion is supposed to have uniform spectrum to examine the frequency transfer function of the model directly.

Figure 2. shows the mean of the cross spectral matrix of acceleration response in the x direction between node 34 and node 38. The (1,1) component is the auto spectral function of the response at node 34, the (2,1) component is the cross spectral function of the response between node 24 and node 38, and the (2,2) component is the auto spectral function of the response at node 38. In the same manner, Figure 3. shows the square root of the variance (the standard deviation or σ) of the cross spectral matrix of the response between node 34 and node 38.

The first dominant frequency of the model is about 1.8(Hz) and the peak value of the function (the (2,2) component corresponds to node 38) is about 8.5. The (2,2) component in Figure 3. shows a typical variation along frequency axis with two peaks before and after the dominant frequency(1.8(Hz)). The maximum value of the standard deviation is about 0.42 which is about 5(%) of the mean peak value.

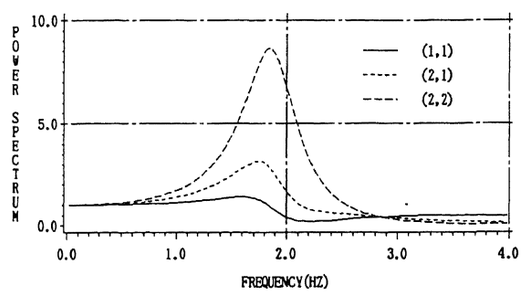

Figure 2. The mean of the cross spectral matrix of response.

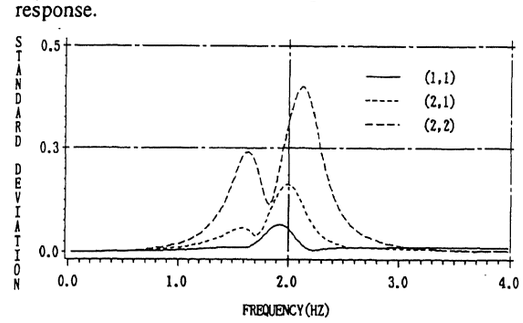

Figure 3. The standard deviation of the cross spectral matrix of response.

Next to show the approximation performance of the proposed method, Monte-Carlo simulation was carried out using our original analysis code called *VESLDYN* which can perform a reliable deterministic frequency response analysis just the same as SUPERFLUSH. The same analytical model in size as the above without free fields was used to let the resonance easily take place so that effectiveness of the proposed method can be directly examined. Boundaries are supposed to be horizontal rollers.

Figure 4. shows the change of the frequency response function at node 38 in the x direction along Young's modulus of material 1 by Monte-Carlo simulation. The number of trials is 15. Each line shows a section of the three dimensional frequency response function at a certain frequency. Five sections at five frequencies are shown in the figure. We can see the strong non-linearity at 1.5(Hz) and 2.5(Hz) and these variations are quite difficult to be approximated by the perturbation method in which the first or second-order approximation is used. Figure 5. shows the

corresponding interpolation functions by the proposed method. Each interpolation function was determined using only the mean and the first-order derivative just the same as the stochastic finite element method using the perturbation method. The interpolation function at frequency 1.5(Hz) shows a quite good agreement with the corresponding one in Figure 4., but the function at frequency 2.5(Hz) does not show a good agreement. This is a kind of limitation of the proposed method because the method is based on the frequency response function of a SODF system. To check the degree of the agreement, the integral of $|H(\omega)|f(E)$ over from 0.0(Hz) to 5.0(Hz) and from -3.5σ to 3.5σ are summarized in Table 2. The difference between the two in the Table is about 1.2(%) or less. This may show a good performance of approximation in the proposed method.

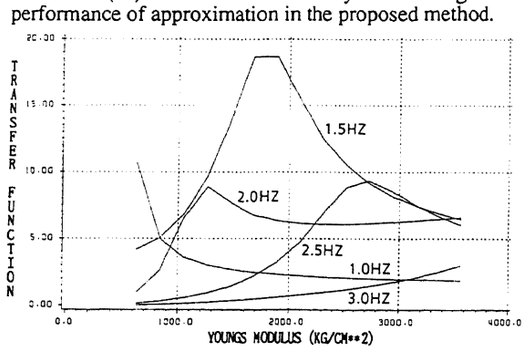

Figure 4. The change of the frequency transfer function by Monte-Carlo simulation (Young's modulus axis).

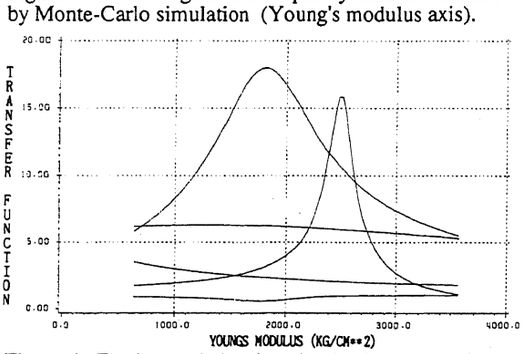

Figure 5. The interpolation function by the proposed method (Young's modulus axis).

Table 2. Comparison the proposed method with Monte-Carlo simulation.

Degree of freedom	Monte-Carlo (A)*	Proposed method (B)*	|A - B|/A x100 (%)
node 34 x - dir.	3.3089 x10^3	3.3168 x10^3	0.242
node 34 y - dir.	1.5664 x10^3	1.5767 x10^3	0.658
node 38 x - dir.	5.9490 x10^3	6.0188 x10^3	1.173
node 38 y - dir.	1.6301 x10^3	1.6419 x10^3	0.724

* These values are $\int\int |H(\omega)| f(E)\, d\omega\, dE$.

3.2 *Parametric study on a practical model*

The finite element model which consists of 144 elements and 165 nodes in this numerical example is shown in Figure 6. Analytical area is 1600.0(m) in width and 400.0(m) in depth. The free field consist of 10 layers. As is shown in the figure, the analytical model is a half model using the symmetric condition at the center of the area.

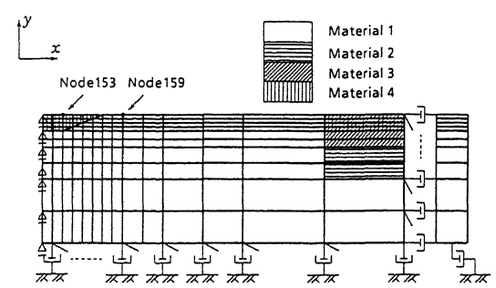

Figure 6. Practical finite element model.

Table 3. Material properties in the practical model.

Material No.	Young,s modulus (kN/m^2)	Poisson's ratio	Unit mass (kg/m^3)	Damping factor
1	2.60x10^7 (0.2)	0.3 (0.2)	2.5x10^3 (0.05)	0.03 (0.4)
2	6.44x10^6 (0.2)	0.4 (0.2)	2.3x10^3 (0.05)	0.05 (0.4)
3	1.61x10^6 (0.2)	0.4 (0.2)	2.3x10^3 (0.05)	0.05 (0.4)
4	3.63x10^5 (0.2)	0.45 (0.2)	2.0x10^3 (0.05)	0.10 (0.4)

The model has four materials. Used material properties are summarized in Table 3. These values are supposed to be practical one including COV. Young's modulus and the unit mass are determined so that the shear wave velocity (V_S) in each material become 2000.0(m/s), 1000.0, 500.0 and 250.0 respectively. Four kinds of random variables are also considered in this example. The values in the parentheses are the coefficient of variations(COV) which is also determined to be practical. COVs in the free field are supposed to be 0.05. The total number of the random variables are 616. Correlation among the random variables is evaluated by the exponential model with the parameter α=0.02(1/m) and β=0.1(1/m). This means correlation coefficient becomes 1/e at the distance 50(m) in the x direction and it becomes 1/e at the distance 10(m) in the y direction. This is because material properties show, in general, higher correlation in the x direction than in the y direction. Correlation is only evaluated among the same material and the same property.

In the same way as the basic numerical example above, input motion is supposed to have an uniform spectrum to examine the frequency transfer function of the model directly. In the same manner as the above

example, Figure 7. shows the mean of the cross spectral matrix of acceleration response in the x direction between node 153 and node 159. The (1,1) component is the auto spectral function of the response at node 153, the (2,1) component is the cross spectral function of the response between node 153 and node 159, and the (2,2) component is the auto spectral function of the response at node 159. In the same manner, Figure 8. shows the square root of the variance (the standard deviation) of the cross spectral matrix of the response between node 153 and node 159.

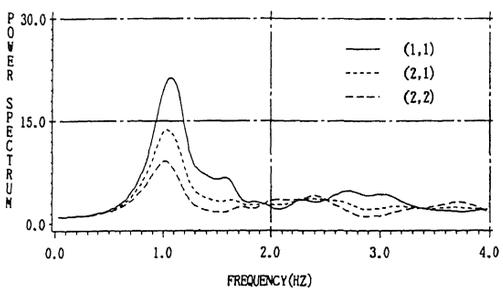

Figure 7. The mean of the cross spectral matrix of response.

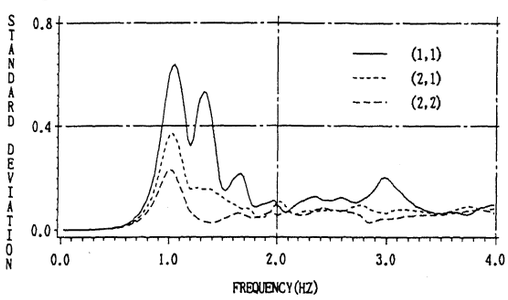

Figure 8. The standard deviation of the cross spectral matrix of response.

The first dominant frequency of the model is about 1.1(Hz) and the peak value is about 20.5. Figure 8. shows the peak value of the (1,1) component is about 0.65 which is about 3(%) of the mean peak level. This may be because the correlation parameters employed here are a little smaller. The variation of the overall σ in Figure 8. may have many factors, so direct engineering understanding of the variation is somewhat difficult. The result shows that the change of the mean is so small under the analytical suppositions, so the change of the standard variation of response, which is our main objective, is focused on in this paper. From Figure 9. to Figure 12., the standard deviations of the response to the variation of the four kind of random variables in the irregular zone are shown . Figure 9 shows the σ due to Young's modulus. Figure 10. shows the σ due to the unit mass. Figure 11. is due to Poisson's ratio and Figure 12. is due to the damping factor. The interpolation function for Poisson's ratio and the damping factor is a linear function, but almost no inherent behavior is seen in Figure 11. and 12.

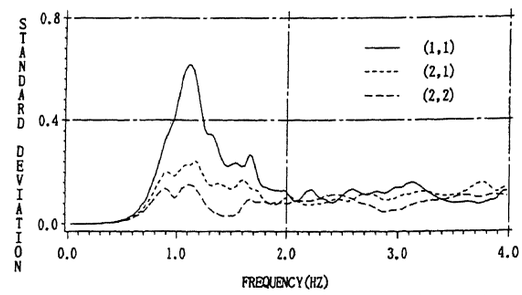

Figure 9. The standard deviation of response due to the change of Young's modulus in the irregular zone.

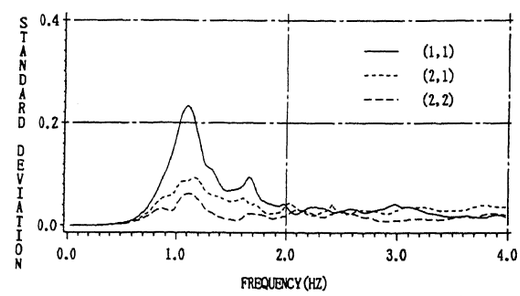

Figure 10. The standard deviation of response due to the change of the unit mass in the irregular zone.

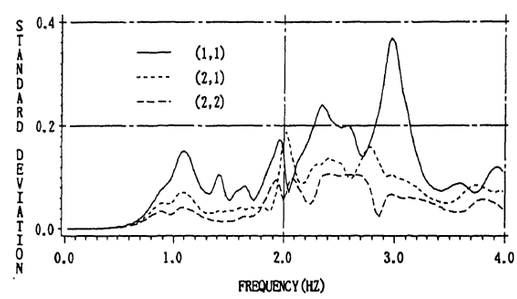

Figure 11. The standard deviation of response due to the change of Poisson's ratio in the irregular zone.

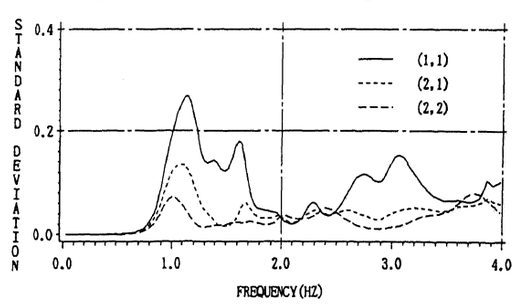

Figure 12. The standard deviation of response due into the change of the damping factor in the irregular zone.

Next to examine the influence by the COV, the COV of Young's modulus in the irregular zone is changed to four level, 0.05, 0.10, 0.20 and 0.30. Figure 13.

shows the σ due to the change of the COV. A kind of linear relation is seen among them in the figure.

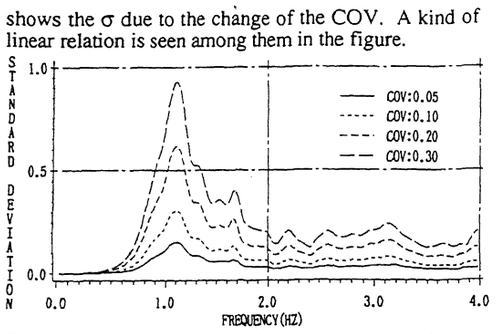

Figure 13. The standard deviation of response due to the change of the COV of Young's modulus.

In the final numerical study, to examine the influence by the location of random variable, the COV of each material is only considered. Figure 14. shows the case Young's modulus in each material in the irregular zone is only random variable. Figure 15. shows the case the unit mass in the irregular zone is only random variable. Figure 16. shows the case Young's modulus in each material in the free field is only random variable. Figure 17. shows the case the unit mass in the free field is only random variable.

Figure 14. and Figure 15. show a change similar to each other except for the change due to the unit mass in material 3. In general, the unit mass far away from the response node does not have a much effect to the response. Figure 16. and 17. show that the σ due to the free field is much bigger than that in the irregular zone.

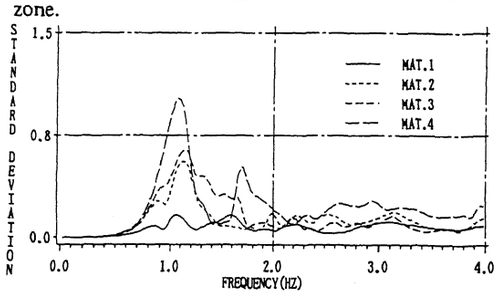

Figure 14. The standard deviation of response due to the change of Young's modulus in the irregular zone.

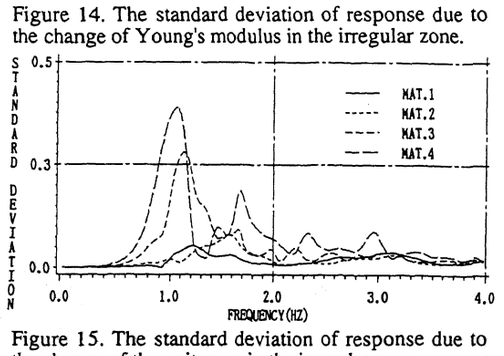

Figure 15. The standard deviation of response due to the change of the unit mass in the irregular zone.

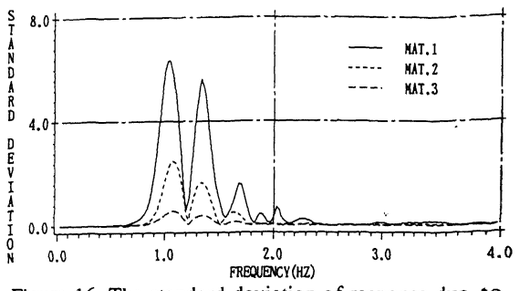

Figure 16. The standard deviation of response due to the change of Young's modulus in the free field.

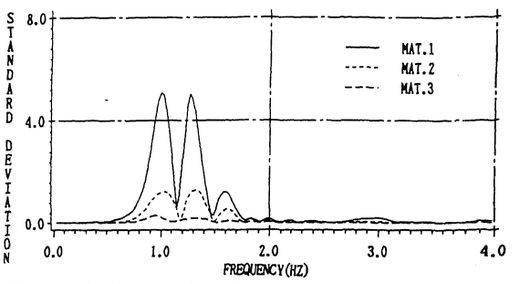

Figure 17. The standard deviation of response due to the change of the unit mass in the free field.

4. CONCLUDING REMARKS

Using the interpolation function method, stochastic evaluation of ground motion of practical model during earthquake was performed in this study through the investigation on the change of the frequency transfer function of the model. However engineering judgement or examination on the numerical results is difficult because there are too many related factors and there is no alternative to check the results except for Monte-Carlo simulation for a simple model. To prove the validity of the proposed method, further investigation may be necessary.

REFERENCES

Crandall, S. and Mark, W. 1963. *Random vibration.* New York: Academic Press.

Hisada, T. and Nakagiri, S. 1981. Stochastic finite element method developed for structural safety and reliability. Proc. of 3rd *ICOSSAR*: p.395.

Hisada, T. and Nakagiri, S. 1985. Role of the stochastic finite element method in structural safety and reliability. Proc. of 4th *ICOSSAR*: I-385.

Lin, Y. 1967. *Probabilistic theory of structural dynamics.* : McGRAW-HILL.

Nigam, N. Introduction to random vibration. : MIT Press.

Ukon, H. et al. 1988. An interpolation function method for stochastic FEM analysis under dynamic loads using frequency response analysis. Structural Eng./Earthquake Eng. *JSCE*: No.392/I-9.

Ukon, H. et al. 1990. Frequency response analysis of probabilistic structures with random viscous boundary. Proc. of 45th annual conference. *JSCE*.